

Hemodynamic Analysis of a Three-Point Suture During Tapering Technique for Microanastomosis Using Computational Fluid Dynamics

Shunjiro Yagi, MD, PhD,* Takafumi Sasaki, PhD,[†] Takahiro Fukuhara, MD, PhD,[‡]
Kaori Fujii, MD,* Maki Morita, MD,* Kohei Fukuoka, MD,* Kento Ikuta, MD,*
Ryunosuke Umeda, MD,* Haruka Kanayama, MD,* and Yoshiko Suyama, MD*

Abstract: The tapering technique is one of the useful methods of anastomosing 2 vessels with large discrepancies during microanastomoses. When the tapering technique is used, a three-point suture is always present. The authors analyzed the most appropriate suture technique for this using computational fluid dynamics. This aspect has not previously been addressed. Three different suture techniques were simulated: (1) Three single-knot sutures (Type I); (2) Two single-knot sutures forming an X-shape (Type II); and (3) A single continuous ligature through the vascular wall (Type III).

Vascular models of these 3 types were created. The streamline, wall shear stress, and oscillatory shear index at the anastomosis site were measured using a previously prepared venous model. Streamline disruption was most severe for Type II. In all 3 types, the highest wall shear stress was recorded at the suture peak protruding into the vessel. The maximum oscillatory shear index was highest in Type II, and lowest in Type III. The present results suggest that Type III is the best three-point suturing method for the tapering technique.

Key Words: Computational fluid dynamics, free flap, microanastomosis, microsurgery, tapering technique

(*J Craniofac Surg* 2021;32: 2749–2752)

Although microsurgery has become a common procedure,^{1,2} the choice of the technique still depends on microsurgeons' experience rather than evidence. The tapering technique is often used when microsurgeons perform anastomoses of the vessels with large

From the *Department of Plastic and Reconstructive Surgery, Tottori University Hospital, Yonago 683-8504, Japan; [†]Cardio Flow Design, Inc., Chiyoda, Tokyo; and [‡]Division of Otolaryngology, Head and Neck Surgery, Department of Sensory and Motor Organs, School of Medicine, Faculty of Medicine, Tottori University, Yonago, Japan.

Received April 12, 2021.

Accepted for publication May 4, 2021.

Address correspondence and reprint requests to: Shunjiro Yagi, MD, PhD, Tottori University Hospital, Yonago 683-8504, Tottori, Japan; E-mail: yagishun68@gmail.com

The authors report no conflicts of interest.

This is an open access article distributed under the terms of the Creative Commons Attribution-Non Commercial-No Derivatives License 4.0 (CCBY-NC-ND), where it is permissible to download and share the work provided it is properly cited. The work cannot be changed in any way or used commercially without permission from the journal.

Copyright © 2021 The Author(s). Published by Wolters Kluwer Health, Inc. on behalf of Mutaz B. Habal, MD.

ISSN: 1049-2275

DOI: 10.1097/SCS.00000000000007859

discrepancies.³ The larger-diameter vessel is cut obliquely in a funnel shape. As this portion is sutured together to reduce the vessel diameter, a three-point suture is always present when the vessels are anastomosed. This three-point suture site is susceptible to blood leakage. If the number of sutures is increased to prevent such leakage, there is the risk of thrombosis. Therefore, we compared three different types of suture techniques for the three-point suture site by using computational fluid dynamics (CFD), to evaluate the suture thread's effect from a hemodynamic point of view. From the results, we investigated the effects of each suture thread on blood flow at the microanastomosis site to ascertain the most appropriate method for the three-point suture site.

MATERIALS AND METHODS

We established a model of vascular anastomosis 2 mm in diameter with the suture thread of 0.03 mm diameter. The diameter of the suture thread is equivalent to 10-0 nylon. The three types of sutures to be used at the three-point suture site during the tapering technique were defined (Fig. 1) as follows:

- Three single-knot sutures (Type I)
- Two single-knot sutures forming an X-shape (Type II)
- A single continuous ligature through the vascular wall (Type III)

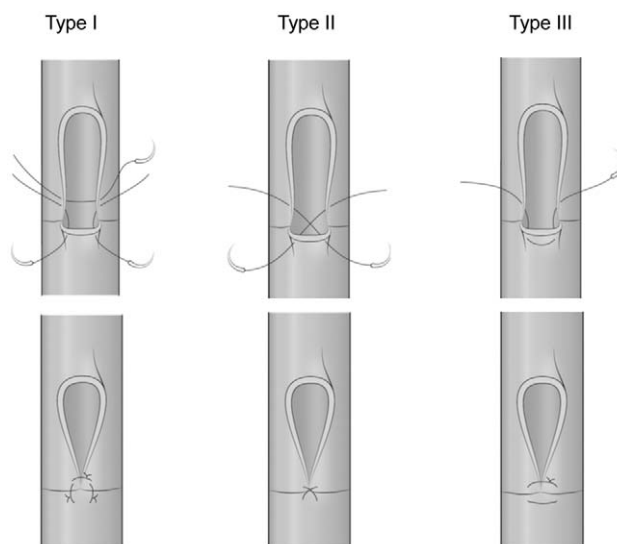


FIGURE 1. Three-point suture techniques. In Type I, the suture is formed by three stitches. In Type II, it is formed by 2 stitches in an X-shape. In Type III, it is formed by a single continuous stitch.

At 10 locations (including a three-point suture), sutures were placed around the junction of the vessels, with the thread extending into the lumen at the height of 0.025 mm and length of 0.115 mm. In Type I, 2 sutures out of three were lined up in parallel with the three-point suture at intervals of 0.015 mm and in Type III, at intervals of 0.05 mm. The height of the crossing threads at the three-point suture in Type II was 0.02 mm. These geometries were constructed by using computer-aided design (CAD) software (Fusion 360, Autodesk, Inc., USA), and the computational meshes were created using commercial meshing software (ANSYS ICEM16.0, ANSYS Japan, Tokyo, Japan). The mesh consisted of 723,211 elements and 201,167 nodes in Type I; 722,622 elements and 201,394 nodes in Type II; and 700,890 elements and 198,467 nodes in Type III (Fig. 2).

Inlet blood flow was created using an ultrasound flowmeter (HT323 surgical flowmeter, Transonic Systems, Ithaca, NY) with a period of 1.0 second, based on the venous waveform.⁴ Inlet blood flow was set up to facilitate 45 mL/min at 0.14 seconds (maximum value), -19.0 mL/min at 0.84 seconds (minimum value), and 13.0 mL/min (mean value) (Fig. 3). The wall surface was given a no-slip condition and the pressure gradient at the outlet was stipulated as zero. OpenFOAM v5.0 software was used for CFD analysis. The turbulent pulsatile flow simulation was performed with reference to previous hemodynamic research. The software solved the Navier–Stokes equations of an incompressible transient Newtonian fluid. We set the time step size up to 5.0 times 10⁻⁵ seconds to reduce the Courant number to a sufficient level, and we set the convergence criteria to 10⁻⁵ which timed the residual at each time step. Blood density was 1,060 kg/m³, the coefficient of viscosity was 0.004 Pa·s to simulate blood.^{5,6} Streamlines (SL), wall shear stress (WSS), and oscillatory shear index (OSI) were visualized and analyzed by using CFD postprocessing software (ParaView, Kitware, NY).

Streamlines is represented by the lines connecting velocity vectors to visualize blood flow directions and vortex structures. WSS is a frequently-used indicator in blood flow research because stress is known to relate to plaque and aneurysm development.⁷ WSS is calculated as a velocity gradient by using longitudinal velocity, distance from the wall, and viscosity. In other words, it is the frictional force exerted by the blood on the vascular wall and measured in Pa (N/m²).⁸ OSI that expresses the changes in the

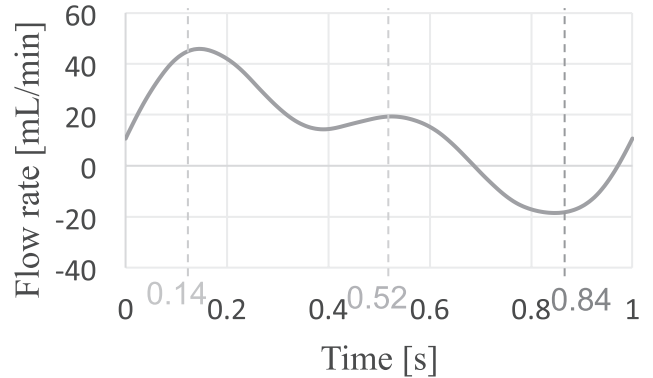


FIGURE 3. Model venous waveform. The period is 1 second, maximum flow is 45.0 mL/min, minimum flow is -19.0 mL/min, and mean flow is 13.0 mL/min.

direction of the WSS. This indicates the degree of direction reversal of the WSS within a single pulse cycle⁹ (Fig. 4).

RESULTS

Streamlines

In Type I, SL disruption was evident near the thread ligated perpendicular to the blood flow at the three-point suture. Disruption of SL flow was similarly evident as it passed through each line of the three sutures on the outlet side. The blood flow rate decreased at each time point (0.14, 0.52, and 0.84 seconds) around the sutures and when the blood passed through the three-point suture site and over the line of the three sutures on the outlet side. SL disruption and a decreased blood flow rate were similarly evident at the three-point suture site and around the line of the three sutures on the outlet side in Type II. The SL disruption around the suture threads as they crossed in an X-shape at the three-point suture in Type II was more severe than that seen in Types I and III. In Type III, some SL disruption was evident at the three-point suture site and around the sutures on the outlet side. However, almost no decrease in the blood flow rate was shown at these sites. The SL of the blood flow passing over the suture threads lined up in parallel with the three-point suture site was also more consistent than in either Type I or II at each time point (0.14, 0.52, and 0.84 seconds) (Fig. 5).

Wall Shear Stress

In all three suture methods, the maximum WSS was recorded at 0.14 seconds, that is the time of maximum blood flow, at the peaks of the exposed suture threads in the lumen. The maximum value was 15.24 Pa in Type I, 21.07 Pa in Type II, and 14.03 Pa in Type III (Fig. 6).

Oscillatory Shear Index

In Type I, an OSI of 0.199 was recorded on the vascular wall at the base of the suture running perpendicular to the blood flow. In

$$OSI = \frac{1}{2} \left[1 - \frac{\left| \int_0^T wss_i dt \right|}{\int_0^T |wssi| dt} \right]$$

FIGURE 4. Formula for calculating the oscillatory shear index (OSI).

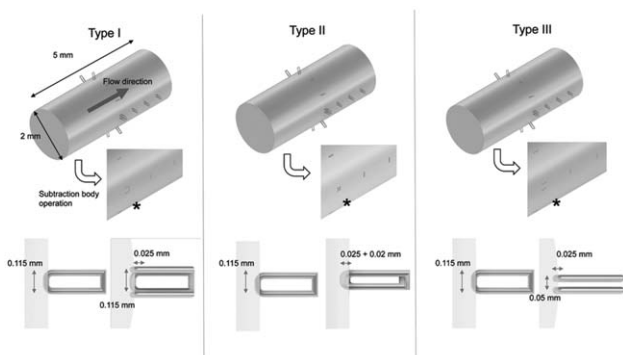


FIGURE 2. Suture modeling process. At 10 locations (including the three-point suture site), sutures are inserted around the circumference of the vessel, with the thread extending into the lumen at a height of 0.025 mm and length of 0.115 mm. In Type I, two sutures of the three are lined up in parallel with the three-point suture at intervals of 0.015 mm, and in Type III at intervals of 0.05 mm. The height of the crossing threads at the three-point suture site in Type II is 0.02 mm. The asterisks (*) indicate the three-point suture sites.

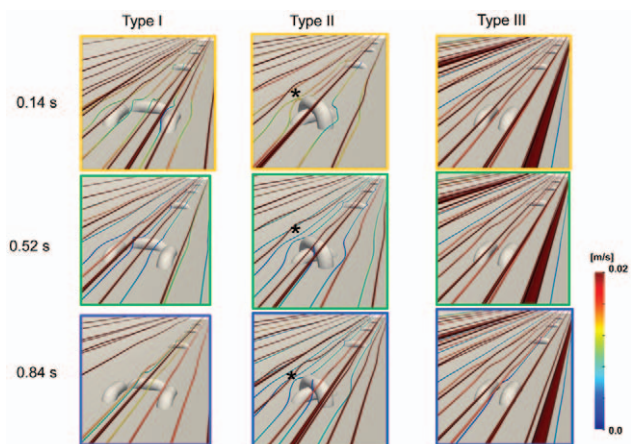


FIGURE 5. Streamline (SL). The blood flow rate decreases at each time point (0.14, 0.52, and 0.84 seconds) when the blood passes through the three-point suture site and over the line of the 3 sutures on the outlet side. The SL disruption around the suture threads that cross in an X-shape at the three-point suture site in Type II is more severe than that seen in Types I and III (asterisks). The SL is smoothest in Type III.

Types II and III, the maximum values recorded at the base of the sutures were 0.206 and 0.193, respectively (Fig. 7).

DISCUSSION

The vessels of microanastomoses in a free flap transfer are usually larger than 1 mm in diameter. Therefore, it is not a technical difficulty. When there are large size differences between the vessels, so that it is not possible to correct the mechanical expansion, the tapering technique is used to solve the problem. In the tapering technique, a three-point suture is necessary where suture threads are crowded. We assumed that the three-point suture site is a predilection site for thrombosis after microanastomoses. In this study, we analyzed which suture method was the most preferred at the three-point suture site when performing the tapering technique, via CFD.

We used a venous model because thrombosis after a microanastomosis occurs more frequently in venous rather than in arterial anastomoses.¹⁰ In this study, CFD analysis was conducted using a model venous waveform. Size discrepancy between the anastomosed vessels may make microanastomoses difficult. The tapering technique³ is used to correct the anastomosing vessels' shape to decrease discrepancy. Although this is an effective technique in the microanastomosis of vessels of different sizes, it creates a three-point suture site. More thread is needed to suture the oblique portion than is used in a conventional end-to-end anastomosis. In this study, a simplified analysis simulating an anastomosis between two

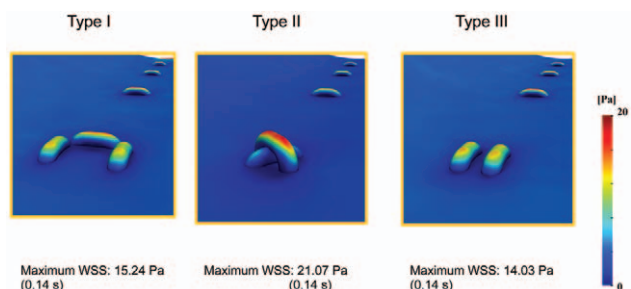


FIGURE 6. Wall shear stress (WSS): The peak value recorded at 0.14 seconds is 15.24 Pa in Type I, 21.07 Pa in Type II, and 14.03 Pa in Type III.

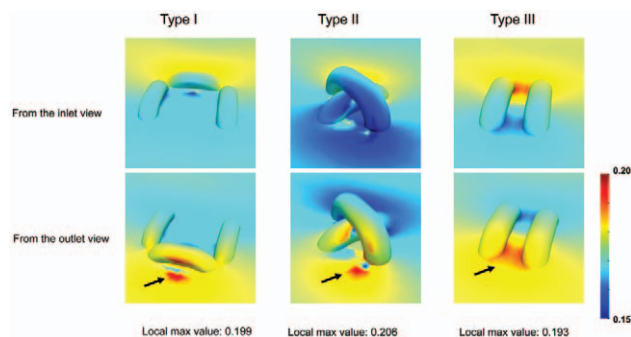


FIGURE 7. Oscillatory shear index (OSI): The peak value is 0.199 in Type I, 0.206 in Type II, and 0.193 in Type III. In all 3 types, the highest OSI is seen at the point where the suture exits the vascular wall (arrows).

vessels of the same diameter was carried out to investigate the effect of the suture threads at the three-point suture site on blood flow. Three different types of the three-point suture were also simulated. Type I required 3 stitches but the threads protrude only a small distance into the vascular lumen. Type II required two stitches and the threads protrude further into the vascular lumen, but blood is less likely to leak from the three-point suture site. Type III consisted of only a single stitch but required continuous needle movement, and it was the most technically difficult of all three ms. Blood is unlikely to leak from the three-point suture site, and the threads protrude only a little way into the lumen, but they are packed closely together. Each of these suture types has its advantages and disadvantages. In this study, it was possible to evaluate their characteristics in terms of fluid dynamics using CFD analysis.

Computational fluid dynamics has been made possible thanks to advances in diagnostic imaging technology and computer simulation techniques. Computational fluid dynamics has been used for analyzing the mechanism including the origin, growth, and rupture of cerebral aneurysms.¹¹⁻¹³ A previous report revealed that microanastomoses using a coupling device showed less SL disruption because coupling devices do not require a suture thread.¹⁴ Our study suggested that SL disruption was the largest for the Type II three-point suture, although SL disruption occurred close to the suture threads on the outlet side and WSS was higher at the microanastomosis using suture threads rather than a coupling device. This suggests that the higher distance to which the thread protruded into the vascular lumen induces SL disruption. Complex or loose knots may cause SL disruption because of the thread protruding further into the lumen.

Wall shear stress prevents the occurrence of thrombosis. Wall shear stress is a force that acts at a tangent to the vessel wall which would remove clots, even if thrombosis was to begin to form.¹⁵ As friction between the vascular wall and the blood flow reduces the blood flow rate near the vascular wall, the highest value of the WSS was recorded at the peak of the threads used for the Type II three-point suture, which was furthest from the vascular wall.

The OSI is another important CFD parameter. A high OSI has been implicated in the generation of oxygen free radicals.¹⁶ Vascular endothelial cells receive severe oxidative stress during post-ischemic reperfusion.¹⁷ Damage to vascular endothelial cells by oxygen free radicals is likely related to the formation of thrombosis. In all three methods of three-point sutures, the OSI was highest near the base of the suture threads. The area close to the base of the thread is therefore susceptible to the formation of thrombosis. Since the flow of venous blood reverses with the beating of the pulse, during the retrograde phase, it collides with the anastomosis, generating eddies. This flow pattern may be why the value was

comparatively high on the outlet side. Arterial blood generally flows in one direction, and therefore, the OSI should be comparatively lower at arterial anastomoses than at venous anastomoses. This situation may be one factor that increases the likelihood of thrombosis formation at venous microanastomoses than at arterial microanastomoses.

CONCLUSIONS

Computational fluid dynamics analysis of the three-point suture site during the tapering technique showed that SL disruption was greatest for Type II. In all 3 suture types, the OSI was highest near the vascular wall at the three-point suture site. The OSI was highest in Type II and lowest in Type III. These results suggest that Type III is the optimum three-point suture method for the tapering technique.

In a native vessel, these parameters of fluid mechanics are like a straight tube and should be almost the same in space. As mentioned above, some research studies have indicated the different distribution of SL, WSS, and OSI effects in some biological situations. Around these anastomoses, there are different distributions of indicators and in this study, we investigated how they affected the suture types.

ACKNOWLEDGMENTS

This research was supported by a grant from the research fund granted by the director of Tottori University, Faculty of Medicine.

REFERENCES

1. Yagi S, Nakayama B, Kamei Y, Takahashi M, Torii S. Posterolateral cervical vein as a recipient vein in reconstructive microvascular surgery of the head and neck. *J Reconstr Microsurg* 2007;23:19–23
2. Yagi S, Kamei Y, Fujimoto Y, Torii S. Use of the internal mammary vessels as recipient vessels for an omental flap in head and neck reconstruction. *Ann Plast Surg* 2007;58:5631–5635
3. Ryan AD, Goldberg I, O'Brien BM, et al. Anastomosis of vessels of unequal diameter using interpositional vein graft. *Plast Reconstr Surg* 1988;81:414–417
4. Yagi S, Sasaki T, Fukuhara T, et al. Hemodynamic analysis of a microanastomosis using computational fluid dynamics. *Yonago Acta Med* 2020;63:308–312
5. Itatani K, Miyaji K, Qian Y, et al. Influence of surgical arch reconstruction methods on single ventricle workload in the Norwood procedure. *J Thorac Cardiovasc Surg* 2012;144:130–138
6. Miyazaki S, Miyaji K, Itatani K, et al. Surgical strategy for aortic arch reconstruction after the Norwood procedure based on numerical flow analysis. *Interact Cardiovasc Thorac Surg* 2018;26:460–467
7. Samady H, Eshtehardi P, McDaniel MC, et al. Coronary artery wall shear stress is associated with progression and transformation of atherosclerotic plaque and arterial remodeling in patients with coronary artery disease. *Circulation* 2011;124:779–788
8. Malek AM, Alper SL, Izumo S. Hemodynamic shear stress and its role in atherosclerosis. *JAMA* 1999;282:2035–2042
9. He X, Ku DN. Pulsatile flow in the human left coronary artery bifurcation: average conditions. *J Biomech* 1996;118:74–82
10. Hyodo I, Nakayama B, Kato H, et al. Analysis of salvage operation in head and neck microsurgical reconstruction. *Laryngoscope* 2007;117:357–360
11. Misaki K, Takao H, Suzuki T, et al. Estimated pretreatment hemodynamic prognostic factors of aneurysm recurrence after endovascular embolization. *Technol Health Care* 2017;25:843–850
12. Yosiki K, Misaki K, Nambou I, et al. Intraoperative rupture of unruptured cerebral aneurysm during craniotomy: A case report. *Case Rep Neurol* 2017;9:261–266
13. Kamide T, Misaki K, Nambou I, et al. Delayed asymptomatic coil migrations toward different arteries after aneurysmal embolization: case report 2017. *Acta Neurochir (Wien)* 2017;159:593–598
14. Wain RA, Whitty JP, Dalal MD, Holmes MC, Ahmed W. Blood flow through sutured and coupled microvascular anastomoses: A comparative computational study. *J Plast Reconstr Aesthetic Surg* 2014;67:951–959
15. Maruyama O, Kosaka R, Nishida M, et al. In vitro thrombogenesis resulting from decreased shear rate and blood coagulability. *Int J Artif Organs* 2016;39:194–199
16. Hwang J, Saha A, Boo YC, et al. Oscillatory shear stress stimulates endothelial production of from p47phox-dependent NAD(P)H oxidases, leading to monocyte adhesion. *J Biol Chem* 2003;278:47291–47298
17. Moens AL, Claeys MJ, Timmermans JP, Vrints CJ. Myocardial ischemia/reperfusion-injury, a clinical view on a complex pathophysiological process. *Int J Cardiol* 2005;100:179–190